THE JOURNAL OF PHYSICAL CHEMISTRY A

Article

pubs.acs.org/JPCA

Simulations of the Ultrafast Transient Absorption Dynamics of a Donor−Acceptor Biaryl in Solution

Roman G. Fedunov,[†] Anastasiia V. Plotnikova,[†] Anatoly I. Ivanov,*[,†] and Eric Vauthey*[,‡]

[†]Volgograd State University, University Avenue 100, Volgograd 400062, Russia

[‡]Department of Physical Chemistry, University of Geneva, 30 quai Ernest-Ansermet, CH-1211 Geneva 4, Switzerland

ABSTRACT: A model for simulating the transient electronic absorption spectra of donor−acceptor dyads undergoing ultrafast intramolecular charge transfer in solution has been developed. It is based on the stochastic multichannel point-transition approach and includes the reorganization of high-frequency intramolecular modes (treated quantum mechanically) and of low frequency intramolecular and solvent modes (described classically). The relaxation of the slow modes is assumed to be exponential with time constants taken from experiments. The excited-state dynamics is obtained by simulating the population distribution of each quantum state after optical excitation and upon electronic and vibrational transitions. This model was used to simulate the transient electronic absorption spectra measured previously with a pyrylium phenolate in acetonitrile. A very good agreement between the simulated and measured spectra was obtained assuming a three-level model including the ground state, the optically excited state, and a dark state with large charge-transfer character and a substantially different geometry relative to that of the optically excited state. The merit of this approach to disentangle the contributions of both population changes and relaxation processes to the ultrafast spectral dynamics will be discussed.

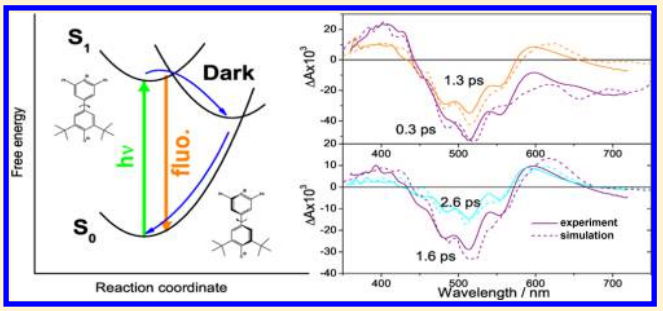

INTRODUCTION

Pyridinium and pyrylium phenolates are electron donor−acceptor biaryls, which have attracted considerable interest as model systems for studying photoinduced intramolecular charge-transfer processes or as molecular platforms for the development of environment sensitive probes or nonlinear optical materials.[1−6] Most of these compounds are characterized by a lack of fluorescence that points to a short excited-state lifetime. The first ultrafast spectroscopic measurements have been performed with betaine-30 (Figure 1), probably the best known representative of this family, by Barbara and co-workers using one-color pump−probe experiments.[7−15] They confirmed ultrafast nonradiative deactivation of the first singlet excited state and pointed to a strong entanglement of this process with solvent relaxation.[7−9] This conclusion was based on the observation of a slowing down of the deactivation dynamics upon decreasing temperature and upon going to solvents with longer relaxation times.[7−9] The observed dynamics were discussed in terms of a two-state model, zwitterionic ground state and weakly polar excited state, using a modified version of the Sumi−Marcus model, the so-called hybrid model, where high-frequency intramolecular modes are treated quantum-mechanically. More recent experiments on betaine-30 using broadband transient electronic absorption spectroscopy revealed that, additionally to solvent relaxation, the dynamics of this process also involve substantial reorganization of intramolecular modes.[11−13] Subsequent measurements on other pyridinium phenolates and on one pyrylium phenolate (PP, Figure 1) using a combination of time-resolved fluorescence and transient absorption (TA) spectroscopies showed that the decay of the optically populated excited state back to the ground state involves a dark intermediate, radiatively decoupled from the ground state.[14−16] From the viscosity dependence of the fluorescence lifetime in polar and apolar solvents, this dark transient was suggested to have a

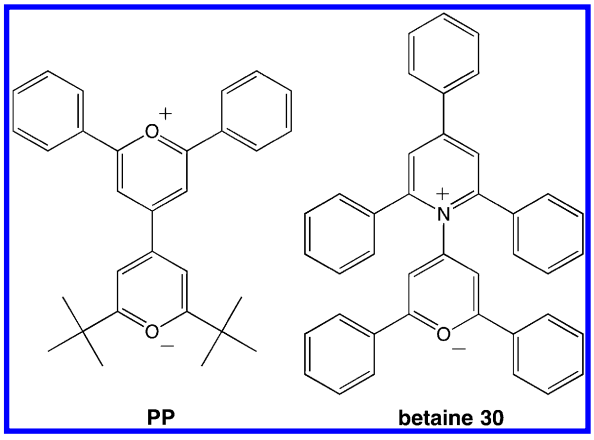

Figure 1. Structure of the pyrylium phenolate PP and of betaine-30.

Received: November 17, 2016
Revised: December 23, 2016
Published: December 23, 2016

DOI: 10.1021/acs.jpca.6b11581
J. Phys. Chem. A 2017, 121, 471−481

twisted geometry with the dihedral angle between the donor and acceptor rings close to 90°. After electronic transition to the ground state in the twisted configuration, the molecules relaxes to the original planar conformation. Betaine-30 and more generally pyridinium phenolates are characterized by a strong solvatochromism, due to the zwitterionic character of their ground, S_0, state and the small electric dipole moment of their first excited, S_1, state.[7−10] Consequently, the $S_1 \leftarrow S_0$ absorption band is broad and structureless as expected for a charge-transfer transition. However, the $S_1 \leftarrow S_0$ absorption band of PP shows only a modest solvatochromism and is characterized by a distinct vibronic structure. There two features point to a weak charge transfer character of this transition.[16]

Deeper insight into the excited-state dynamics of these molecules could in principle be obtained from a more quantitative analysis of the TA data. The standard approach to interpret such data is to perform a global analysis using a sum of exponential functions or assuming a target kinetic model.[17] Although useful, this approach is limited to reaction schemes where each step follows an exponential kinetics. Moreover, it does not allow simulations of transient spectra themselves. The latter requires applying a proper theoretical model. Although the formal theory of pump−probe experiments is well developed,[18−22] its application to the interpretation of ultrafast photochemical processes in real systems encounters severe difficulties. Ultrafast chemical transformations, like those involved in the above-discussed donor−acceptor dyads, occur in parallel to intramolecular and solvent relaxation processes.[23] Therefore, a theory accounting for such nonequilibrium dynamics is needed. The theories of chemical reactions are usually focused on the calculation of the reaction rate constant,[24−27] whereas time-dependent distribution functions over all the states of the system are needed to simulate the TA spectra. Several approaches for describing the influence of the chemical transformation on the transient signals have been developed.[20,28−37] Promising approaches to simulate TA spectra based on quantum-chemical calculations have been recently developed.[38−40] The attosecond dynamics of the electronic density for both the pump and probe response were treated using real time TD-DFT approaches.[38] Both linear and quadratic response functions were used to obtain excitation energies and transition dipole moments between two non-reference states to analyze the contribution of excited-state absorption to the TA spectra.[39] A dissipative extension of the RT-TDDFT method, OSCF2, was applied to simulate the TA spectra of pyrazole and a GFP-chromophore derivative.[40] Although in these approaches, the TA spectra are simulated from first-principle, empirical information has sometime to be included. The main difficulty of all these approaches concern the description of the reorganization of intramolecular vibrational modes of high frequency, which is often ignored, although it may be of paramount importance. Another problem arises when the long-time dynamics have to be simulated. For charge-transfer processes, such a problem exists when the dynamics is investigated in solvents with several strongly different relaxation times.

The multichannel point-transition stochastic model[41−44] operates with time-dependent distribution functions and is, therefore, well suited for the simulation of TA spectra. The model includes physical parameters that can be borrowed from independent experiments. A larger part of these parameters are used to control reaction rates and product yields. The advantage of the model is its ability to predict how the parameters should be varied to get the desired products. The stochastic model can include the reorganization of several high-frequency intramolecular vibrational modes and can describe non-Markovian medium relaxation in terms of several Debye relaxation modes. This model was shown to adequately describe most of the trends found with the dynamics of ultrafast electron transfer reactions in liquids.[45−48] The most important among them are (i) the model predicts a solvent-controlled regime in the Marcus normal region and its almost full suppression in the Marcus inverted region as well as the continuous transition between these behaviors in the vicinity of the activationless region, (ii) in the inverted region, the multichannel stochastic model predicts the apparent activation energy to be much smaller than that calculated with the Marcus equation[49] in full accordance with experimental data,[50−54] (iii) it accounts for the absence of the Marcus normal region in the charge recombination of excited donor−acceptor complexes,[46] and (iv) it reproduces the nonequilibrium two-humped kinetics of the charge separated state population observed with porphyrin-imide dyads upon optical population of the second excited state.[55]

We present here an application of the multichannel point-transition stochastic model to simulate the transient electronic absorption spectra measured after optical excitation of PP in acetonitrile. The choice of this compound instead of the above-discussed zwitterionic pyridinium phenolates was motivated by its structured $S_1 \leftarrow S_0$ absorption band, allowing extraction of important parameters for the simulations. One aim of these simulations is to establish whether the model initially proposed to rationalize excited-state dynamics of PP and similar compounds and invoking a twisted intermediate can indeed account for the observed temporal evolution of the TA spectra. Although this dark intermediate is spectroscopically silent, its involvement manifests indirectly in the TA dynamics. Indeed, the TA spectra of these compounds contain information on the population dynamics of the optically excited state and of the ground state and on how the electronic energy is dissipated and distributed into the high and low frequency nuclear degrees of freedom.

Barbara and co-workers used a two-level model to rationalize the excited-state dynamics of betaine-30. We will show below that such model does not allow the TA spectra of PP to be properly reproduced. The subsequent studies on betaine-30 and other similar biaryls pointed to a strongly nonparabolic excited-state potential along the reaction coordinate. To account for this, we will assume a three-level model that includes the ground state, the optically excited state, and a dark electronic state. For convenience, we call the optically excited state S_1 state, as it is the first excited state observed in the absorption spectrum. The dark state is assumed to be between the S_0 and the S_1 states. As PP is a donor−acceptor biaryl, a considerable charge transfer is expected to accompany the transition from the S_1 to the dark state.[16] This means that, contrary to the transition from the ground to the Franck−Condon S_1 state, this transition to the dark state can involve a large reorganization energy of the solvent and of low-frequency intramolecular modes.

The aims of this paper are (i) to develop a model of a donor−acceptor dyad in solution undergoing ultrafast charge transfer and to simulate its TA dynamics, (ii) to elaborate a computer code for such simulations, (iii) to quantitatively compare theoretical predictions with the experimental data

DOI: 10.1021/acs.jpca.6b11581
J. Phys. Chem. A 2017, 121, 471−481

obtained with PP in acetonitrile,[16] and (iv) to obtain deeper insight into the mechanism responsible for the ultrafast nonradiative decay of the excited state of PP and of similar donor−acceptor biaryls.

THEORY AND COMPUTATIONAL DETAILS

The excited-state dynamics of the donor−acceptor dyad can be depicted as follows:[11,56]

$$\begin{aligned}(\mathrm{DA})_{\mathrm{g}} &\xrightarrow{h\nu} (\mathrm{DA})_{\mathrm{e}}^{*\mathrm{FC}}\\ &\xrightarrow[\text{solvation}]{\text{CVRCT}} (\mathrm{D}^{+}\mathrm{A}^{-})_{\mathrm{d}}^{\mathrm{hot}}\\ &\xrightarrow[\text{solvation}]{\text{CVRCR}} (\mathrm{DA})_{\mathrm{g}}^{\mathrm{hot}}\\ &\xrightarrow[\text{solvation}]{\text{CVR}} (\mathrm{DA})_{\mathrm{g}}^{\mathrm{eq}}\end{aligned} \tag{1}$$

where DA and $D^{+}A^{-}$ designate the states before and after charge transfer, respectively, and the subscripts g, e, d, stand for ground, excited (S_1), and dark state. In principle, DA can be more ionic than $D^{+}A^{-}$. Photoexcitation of the dyad in the thermalized ground state leads to the population of the Franck−Condon (FC) S_1 state (Figure 2). This triggers several

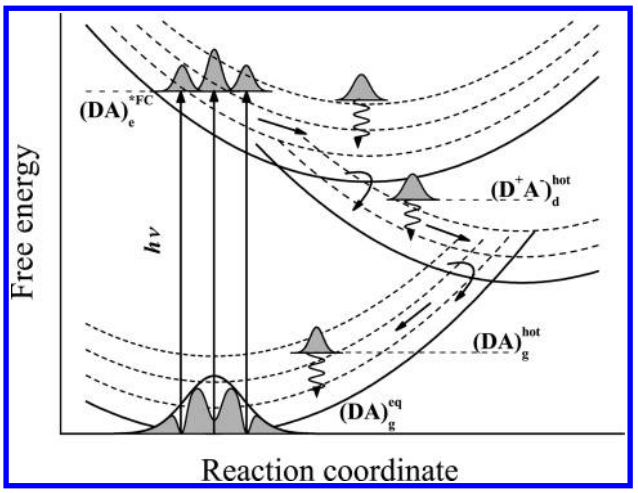

Figure 2. Schematic representation of free energy curves used to model the excited-state dynamics of PP. The dashed lines are the vibrational sublevels of the ground, excited, and dark electronic states. The straight and wavy arrows represent the relaxation of low and high frequency modes, respectively. The population densities after pump pulse on various sublevels are shown as gray areas.

competing processes: solvation, structural relaxation as well as relaxation of high frequency intramolecular modes (CVR), and charge transfer (CT) to the dark electronic state. Directly after CT, the dark state is vibrationally hot and, therefore, charge recombination (CR) to the vibrationally hot ground state occurs in parallel to its relaxation. Finally, the hot ground state relaxes back to thermal equilibrium.

Solvation in acetonitrile occurs on several time scales and can be described by the solvent relaxation function, $X(t)$, which is expressed as a sum of exponential functions[57−59]

$$X(t) = \sum_{i=1}^{N} x_i\, \mathrm{e}^{-t/\tau_i} \tag{2}$$

where x_i, τ_i are the weight and relaxation time constant of the ith solvent mode, respectively, and N is the number of modes. Structural changes of the dyad, like, e.g., torsion around the bond between the donor and acceptor subunits, can be represented as an overdamped low-frequency intramolecular mode and can be included in the relaxation function $X(t)$.

Three parabolic curves for the ground, excited, and dark electronic states with vibrational manifolds will be used to represent the excited-state dynamics of the dyad within the linear dielectric response approximation (Figure 2). A fourth state, h, is needed to account for the excited state absorption observed in the TA experiments.[16]

The reaction coordinate is essentially associated with the low frequency modes (i.e., solvation and structural changes). The motion along Q_i corresponds to the relaxation of the ith mode. The diabatic free energy of the different electronic states along the coordinates Q_i can be expressed as[41,42]

$$U_{\mathrm{g}}^{(n)} = \sum_{i=1}^{N} \frac{Q_i^{\,2}}{2} + \sum_{n} n\hbar\Omega + \Delta G_{\mathrm{eg}} \tag{3}$$

$$U_{\mathrm{e}}^{(m)} = \sum_{i=1}^{N} \frac{(Q_i - \sqrt{2E_{\mathrm{rei}}})^2}{2} + \sum_{m} m\hbar\Omega \tag{4}$$

$$U_{\mathrm{d}}^{(l)} = \sum_{i=1}^{N} \frac{(Q_i - \sqrt{2E_{\mathrm{rdi}}})^2}{2} + \sum_{l} l\hbar\Omega + \Delta G_{\mathrm{ed}} \tag{5}$$

$$U_{h}^{(k)} = \sum_{i=1}^{N} \frac{(Q_i - \sqrt{2E_{\mathrm{rhi}}})^2}{2} + \sum_{k} k\hbar\Omega + \Delta G_{\mathrm{eh}} \tag{6}$$

where ΔG_{ej} is the free energy difference between the S_1 state (state e) and the jth electronic state (j = g, d, h), n, m, l, and k are the quantum numbers of the high-frequency intramolecular mode of frequency Ω, $E_{rji} = x_i E_{rmj}$ is the reorganization energy of ith slow relaxation mode for the transition between the jth and the ground electronic state, and E_{rmj} is the total reorganization energy of the slow modes for the same electronic transition.

In the framework of the stochastic point-transition approach,[42,43,60] the temporal evolution of the system is described by a set of equations for the probability distribution functions in each vibronic states, $\rho_{\mathrm{g,e,d}}^{(n,m,l)}(\vec{Q}, t)$,

$$\frac{\partial \rho_{\mathrm{g}}^{(n)}}{\partial t} = \hat{L}_{\mathrm{g}}\rho_{\mathrm{g}}^{(n)} - \sum_{l} k_{\mathrm{gd}}^{(nl)}(\vec{Q})(\rho_{\mathrm{g}}^{(n)} - \rho_{\mathrm{d}}^{(l)}) + \frac{1}{\tau_{\mathrm{vg}}^{(n+1)}}\rho_{\mathrm{g}}^{(n)} - \frac{1}{\tau_{\mathrm{vg}}^{(n)}}\rho_{\mathrm{g}}^{(n)} \tag{7}$$

$$\frac{\partial \rho_{\mathrm{e}}^{(m)}}{\partial t} = \hat{L}_{\mathrm{e}}\rho_{\mathrm{e}}^{(m)} - \sum_{l} k_{\mathrm{ed}}^{(ml)}(\vec{Q})(\rho_{\mathrm{e}}^{(m)} - \rho_{\mathrm{d}}^{(l)}) + \frac{1}{\tau_{\mathrm{ve}}^{(m+1)}}\rho_{\mathrm{e}}^{(m)} - \frac{1}{\tau_{\mathrm{ve}}^{(m)}}\rho_{\mathrm{e}}^{(m)} \tag{8}$$

$$\frac{\partial \rho_{\mathrm{d}}^{(\vec{l})}}{\partial t} = \hat{L}_{\mathrm{d}}\rho_{\mathrm{d}}^{(l)} - \sum_{n} k_{\mathrm{gd}}^{(nl)}(\vec{Q})(\rho_{\mathrm{d}}^{(l)} - \rho_{\mathrm{g}}^{(n)}) - \sum_{m} k_{\mathrm{ed}}^{(ml)}(\vec{Q})(\rho_{\mathrm{d}}^{(l)} - \rho_{\mathrm{e}}^{(m)}) + \frac{1}{\tau_{\mathrm{vd}}^{(l+1)}}\rho_{\mathrm{d}}^{(l)} - \frac{1}{\tau_{\mathrm{vd}}^{(l)}}\rho_{\mathrm{d}}^{(l)} \tag{9}$$

DOI: 10.1021/acs.jpca.6b11581
J. Phys. Chem. A 2017, 121, 471−481

where $\vec{Q}$ is a vector with the components Q_1, Q_2, ..., Q_N, and $\hat{L}_j$ is the Smoluchowski operator describing the diffusion on the U_j diabatic terms with j = g, e, d

$$\hat{L}_j = \sum_{i=1}^{N} \frac{1}{\tau_i}\left[1 + (Q_i - \sqrt{2E_{rji}})\frac{\partial}{\partial Q_i} + \langle Q_i^2\rangle \frac{\partial^2}{\partial Q_i^2}\right] \tag{10}$$

where $\langle Q_i^2 \rangle = k_B T$ is the width of the equilibrium distribution along the ith coordinate.

The electronic transitions between the vibrational sublevels of the S_1 state and a vibrational sublevel of the jth state are described by the Zusman parameters

$$k_{ij}^{(nm)} = \frac{2\pi (V_{ij}^{(nm)})^2}{\hbar}\delta(U_j^{(n)} - U_i^{(m)}) = \frac{2\pi (V_{ij}^{(nm)})^2}{\hbar} \delta(Y_{ij} - Y_{ij}^{(nm)}) \tag{11}$$

where

$$(V_{ij}^{(nm)})^2 = V_{ij}^2 F_{nm},$$

$$F_{nm} = \exp\{-S\} n! m! \left[\sum_{r=0}^{\min(n,m)} \frac{(-1)^{n-r}(\sqrt{S})^{n+m-2r}}{r!(n-r)!(m-r)!}\right]^2,$$

$$S = \frac{E_{rv}}{\hbar\Omega}$$

and where $Y_{ij} = \sum_k Q_k(\sqrt{2E_{rki}} - \sqrt{2E_{rkj}})$ is the collective energetic reaction coordinate, $Y_{ij}^{(nm)} = E_{rmi} - E_{rmj} + \Delta G_{ei} - \Delta G_{ej} + (n - m)\hbar\Omega$ is a point of intersection of the $U_i^{(n)}$ and $U_j^{(m)}$ terms. F_{nm} is the Franck–Condon factor, and $S = E_{rv}/\hbar\Omega$ and E_{rv} are the Huang–Rhys factor and the reorganization energy of the high frequency vibrational mode, respectively. A single-quantum mechanism $n \rightarrow n - 1$ with a rate constant $1/\tau_i^{(n)}$ is assumed for the relaxation of the high frequency mode of the ith electronic state.

To specify the initial conditions, we assume that the pump pulse has a Gaussian temporal shape

$$E(t) = E_0 \exp\left\{i\omega_e t - \frac{t^2}{2\tau_e^2}\right\} \tag{12}$$

and that its duration is short enough to consider the medium as frozen during excitation. The high-frequency vibrational mode is assumed to be initially in the ground state. This allows obtaining the following general expression for the initial probability distribution function on the S_1 state manifold[61]

$$\rho_e^{(m)}(\vec{Q}, t = 0) = AP_m \exp\left\{-\frac{[\hbar\delta\omega_e^{(m)} - \sum\sqrt{2E_{rei}}Q_i]^2\tau_e^2}{2\hbar^2} - \sum\frac{Q_i^2}{2k_B T}\right\} \tag{13}$$

$$P_m = \left[\frac{S^m e^{-S}}{m!}\right]\exp\left\{-\frac{[\hbar\delta\omega_e^{(m)}]^2}{2\sigma^2}\right\} \tag{14}$$

where $\hbar\delta\omega_e^{(m)} = E_{rme} - \Delta G_{eg} + m\hbar\Omega - \hbar\omega_e$, $\sigma^2 = (2E_{rme}k_B T) + \hbar^2\tau_e^{-2}$, and P_m is a factor proportional to the fraction of the excited dyads in the vibrational state m. The factor A depends on the intensity and duration of the pump pulse and is determined by eq 15.

$$W_p = \int \sum_m \rho_e^{(m)}(\vec{Q}, t = 0) \prod_i dQ_i \tag{15}$$

where W_p is the electronic excitation probability of the dyad by the pump pulse. The initial condition for the ground state distribution function, $\rho_g^{(n)}(\vec{Q}, t = 0)$, can be described as the difference

$$\rho_g^{(n)}(\vec{Q}, t = 0) = \delta_{n,0}[\rho_g^{(eq)} - \rho_e^0(\vec{Q}, t = 0)] \tag{16}$$

where $\delta_{n,0}$ is the Kronecker delta function and

$$\rho_g^{(eq)} = \prod_i \frac{1}{\sqrt{\pi k_B T}} \exp\left\{-\frac{Q_i^2}{2k_B T}\right\},$$

$$\rho_e^0(\vec{Q}, t = 0) = \sum_m \rho_e^{(m)}(\vec{Q}, t = 0) \tag{17}$$

are respectively the equilibrium distribution in the ground state and the distribution of the population transferred to the S_1 state.

The system of differential eqs 7–9 with the initial condition eqs 13 and 16 was solved numerically using the Brownian simulation method.[61,62] We run between 10^5 to 10^6 trajectories in order to obtain the necessary convergence of the results. According to this model, the TA signal can be expressed as

$$\Delta A = -A_{SE} + A_{GSA} - A_{BL} + A_{ESA} \tag{18}$$

where

$$A_{i\rightarrow j}(\omega_p, \tau) = \omega_p \sum_n \sum_m F_{nm} \int_{-\infty}^{\infty} \rho_i^{(n)}(\vec{Q}, \tau) \exp\left\{-\frac{[U_i^{(n)} - U_j^{(m)} + \hbar\omega_p]^2}{2\hbar^2\tau_p^{-2}}\right\} \prod_k dQ_k \tag{19}$$

Here the indices $i \rightarrow j$ adopt the values corresponding to the following contributions to the TA spectra (Figure 3): stimulated emission (SE), hot ground-state absorption (GSA), bleach (BL), and excited-state absorption (ESA). In the cases of SE and ESA, the function $\rho_i^{(n)}(\vec{Q},\tau)$ is the population distribution of the excited state. For BL, this function is the depleted population distribution in the ground state, and for GSA, it is the population distribution transferred from the dark state. Here ω_p and τ_p are the carrier frequency and the duration of the probe pulse.

RESULTS AND DISCUSSION

A simple model involving two electronic states (ground and excited) described with harmonic free energy curves along the reaction coordinate has been previously developed to simulate the TA spectra of betaine-30.[56] It was found to predict TA spectra that differ substantially from those observed experimentally.[56] The origin of this discrepancy is the large reorganization energy that had to be used to reproduce the ultrafast nonradiative deactivation of the excited state. The same problem was found here with PP when using such a two-level model. One shortcoming of this model is the parabolic form assumed for the free energy curves along the reaction coordinate. As shown by quantum-chemistry calculations, the

DOI: 10.1021/acs.jpca.6b11581
J. Phys. Chem. A 2017, 121, 471–481

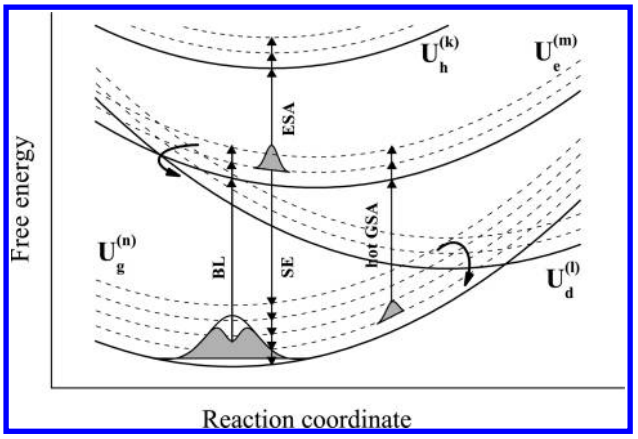

Figure 3. Schematic representation of free energy curves and population densities at time of probe pulse used to simulate the TA spectra of PP with the radiative (vertical arrows) and radiationless transitions (curved arrows). $U_g^{(n)}$, $U_e^{(m)}$, $U_d^{(l)}$, and $U_h^{(k)}$ stand for the ground, excited, dark, and higher excited states, respectively. (BL, bleach; ESA, excited state absorption; GSA, ground state absorption; SE, stimulated emission).

energy profile of the S_1 state of PP along the twist coordinate is far from parabolic.[16] However, the effect of the twist can be accounted for by introducing a third state to the model, namely, a dark state characterized by a high CT character, in agreement with the large torsion angle between the donor and acceptor units of the dyad. Moreover, as this excited twisted state was not directly observed in the TA measurements, its description by a dark state is well justified. Consequently all the simulations presented below were done with the three-level model. These simulations involve a large number of parameters, many of which can be obtained independently. The following parameters for the solvation dynamics ACN were taken from literature:[63] $x_1 = 0.686$, $x_2 = 0.314$ and $\tau_1 = 0.089$ ps, $\tau_2 = 0.63$ ps. The energetic parameters were determined from the analysis of the stationary electronic absorption spectrum of PP in ACN.[16] The free energy change is $\Delta G_{eg} = -2.11$ eV, and the solvent reorganization energy associated with the excitation process amounts to $E_{rme} = 0.11$ eV. The $S_1 \leftarrow S_0$ absorption band exhibits a distinct vibrational progression that points to a single dominant high-frequency Franck–Condon active mode. The parameters deduced for this mode are $\Omega = 0.18$ eV and $E_{rv} = 0.32$ eV. It should be noted that the parameters ΔG_{eg}, E_{rme}, Ω, and E_{rv} impose strong restrictions on the shape and position of stimulated emission, hot ground state absorption, and bleach bands. The other parameters used in the simulations were variable.

The values of the fixed and variable parameters used for the simulations are listed in Tables 1 and 2

Global target analysis of the TA data measured with PP in ACN could be successfully performed assuming two consecutive steps with 0.72 and 4.9 ps time constants.[16] The first step was ascribed to the decay of the S_1 state population and was found to increase with the viscosity of the solvent. Consequently, this decay was associated with the twist around the bond between the donor and acceptor subunit of PP. Since this 0.72 ps time constant is also close to the 0.63 ps relaxation time of ACN, we used the relaxation function of pure ACN for describing the relaxation of the slow nuclear modes. In other words, the reorganization energy, E_{rmd}, includes the reorganization of both the solvent and that related to the twist.[16] The second component with the 4.9 ps time constant was attributed to the back twist of PP in the ground state, i.e., to its structural relaxation from orthogonal to planar equilibrium geometry. Similar twist and back-twist motions have been proposed to account for the spectral dynamics of betaine-30.[11,64] In order to describe this back-twist, a Debye mode with a weight x_3 and a relaxation time constant τ_3 was added to the solvent relaxation function in eq 2. During the fitting procedure, x_3 was free, whereas τ_3 was fixed at $\tau_3 = 4.9$ ps. The relative magnitudes of x_1 and x_2 and the normalization condition, $\sum_{i=1}^{3} x_i = 1$, where conserved.

Since no direct information on the magnitude of the parameters associated with the dark state, namely, the electronic couplings, the free energies, and the reorganization energies, was available, they were considered as free parameters but were restricted to values normally encountered for intramolecular electron transfer processes in polar solvents. For example, the electronic coupling should not strongly exceed k_BT, the solvent reorganization energy should be less than 1 eV, and the dark state should be located between the ground and excited states but closer to the S_1 state.

Experimental TA spectra measured with PP in acetonitrile[16] and simulated ones are depicted in Figures 4–6 (frames A, B, C). Four components can be distinguished in the spectra. The positive signal around 400 nm is due to an excited state absorption (ESA) band. The intense negative band centered around 500 nm originates from the bleach (BL) of the ground-state absorption. The weaker positive feature on the long wavelength side of the bleach arises from hot ground-state absorption (GSA), and the stimulated emission (SE) appear as a negative signal at even longer wavelength, i.e., above 650 nm. The vibrational structure with a frequency of 1450 cm^{-1} (0.18 eV) can be clearly seen at all time delays. The position of BL and its structure depend on the model parameters determined from the stationary absorption spectrum. This BL band is due to the partial depletion of the S_0 population, i.e., "holes". This ensemble of holes is in a nonequilibrium distribution created by the pump pulse. The decay of the BL band depends on the overall relaxation from the other state, whereas its build up is completely determined by the characteristics of the pump pulse. Therefore, the simulation of this band does not require any fit.

The fit starts with the ESA band. The parameters of this band were chosen so that the high energy side of the BL band is partially suppressed. Otherwise, the ratio of the intensities of the BL and SE bands would have been much larger than that observed experimentally. Since the vibrational structure with $\Omega = 0.18$ eV is seen in the overlap region of the ESA and BL bands, the reorganization energy of the low-frequency modes associated with the transition from the S_1 to the upper excited state ($e \rightarrow h$), responsible for the ESA, was assumed to be small as well and was taken as 0.11 eV. In order to properly

Table 1. Fixed Parameters

$x_1/(1-x_3)$	$x_2/(1-x_3)$	τ_1 (ps)	τ_2 (ps)	τ_3 (ps)	ΔG_{eg} (eV)	ΔG_{ed} (eV)	E_{rme} (eV)	E_{rv} (eV)	kT (eV)	Ω (eV)
0.686	0.314	0.089	0.63	4.9	−2.11	−0.9	0.11	0.32	0.025	0.18

DOI: 10.1021/acs.jpca.6b11581
J. Phys. Chem. A 2017, 121, 471–481

Table 2. Variable Parameters

no.	x_3	τ_{vg} (ps)	τ_{ve} (ps)	τ_{vd} (ps)	E_{rmd} (eV)	V_{dg} (eV)	V_{ed} (eV)	E_{rvh} (eV)	ΔG_{eh} (eV)
fitting 1	0.3	0.4	0.05	0.05	0.85	0.036	0.014	0.48	2.49
fitting 2	0.1	0.8	0.05	0.05	0.75	0.036	0.014	0.48	2.49
fitting 3	0.1	1.2	0.05	0.05	0.75	0.036	0.014	0.48	2.49

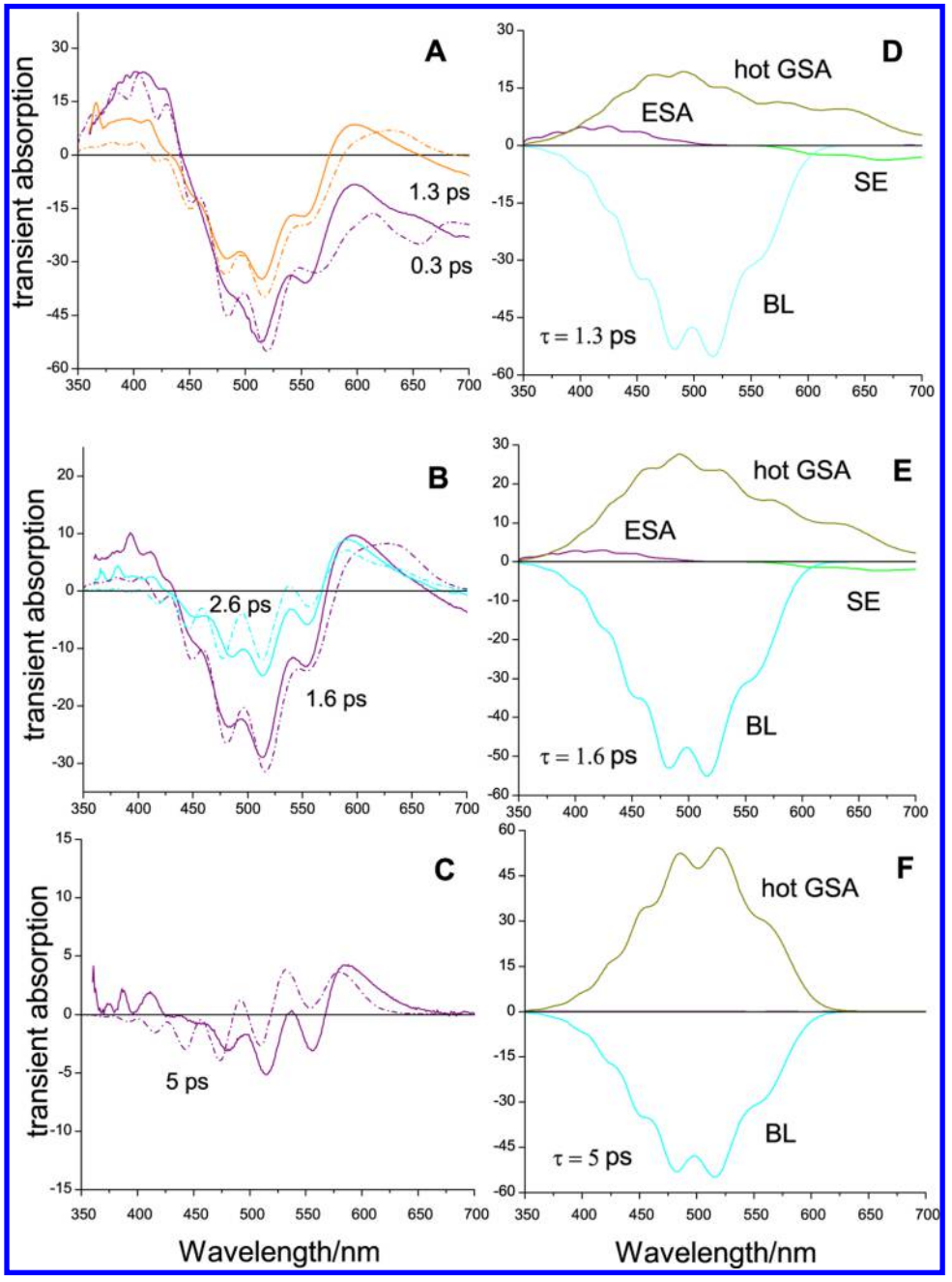

Figure 4. Experimental (solid lines) and simulated (dashed lines) at various time delays after excitation $\Delta A(\lambda)$ (A–C) and their different contributions (D–F). Fitting 1. The parameters are E_{rmd} = 0.85 eV, x_3 = 0.3, τ_{vg} = 0.4 ps.

reproduce the positive feature in the short wavelength region, a reorganization energy of the high-frequency mode of E_{rvh} = 0.48 eV and a free energy gap of ΔG_{eh} = 2.49 eV had to be assumed. A variation of the free energy gap as small as 0.01 eV was sufficient to lead to significant changes in the vibrational structure of the TA spectrum in the 450 nm region.

The decay of the ESA and SE bands is determined by that of the S_1 state population, which itself depends on the electronic coupling, V_{ed}. An excited state lifetime of τ = 0.84 ps, close to that of τ = 0.72 ps found experimentally,[16] was obtained assuming V_{ed} = 0.014 eV.

The hot GSA band is the TA feature that is the most sensitive to the mechanism of the electronic transitions. According to its position, this band is due to molecules in the electronic ground state produced far from the equilibrium of the slowly relaxing modes and in excited states of the high-

DOI: 10.1021/acs.jpca.6b11581
J. Phys. Chem. A 2017, 121, 471–481

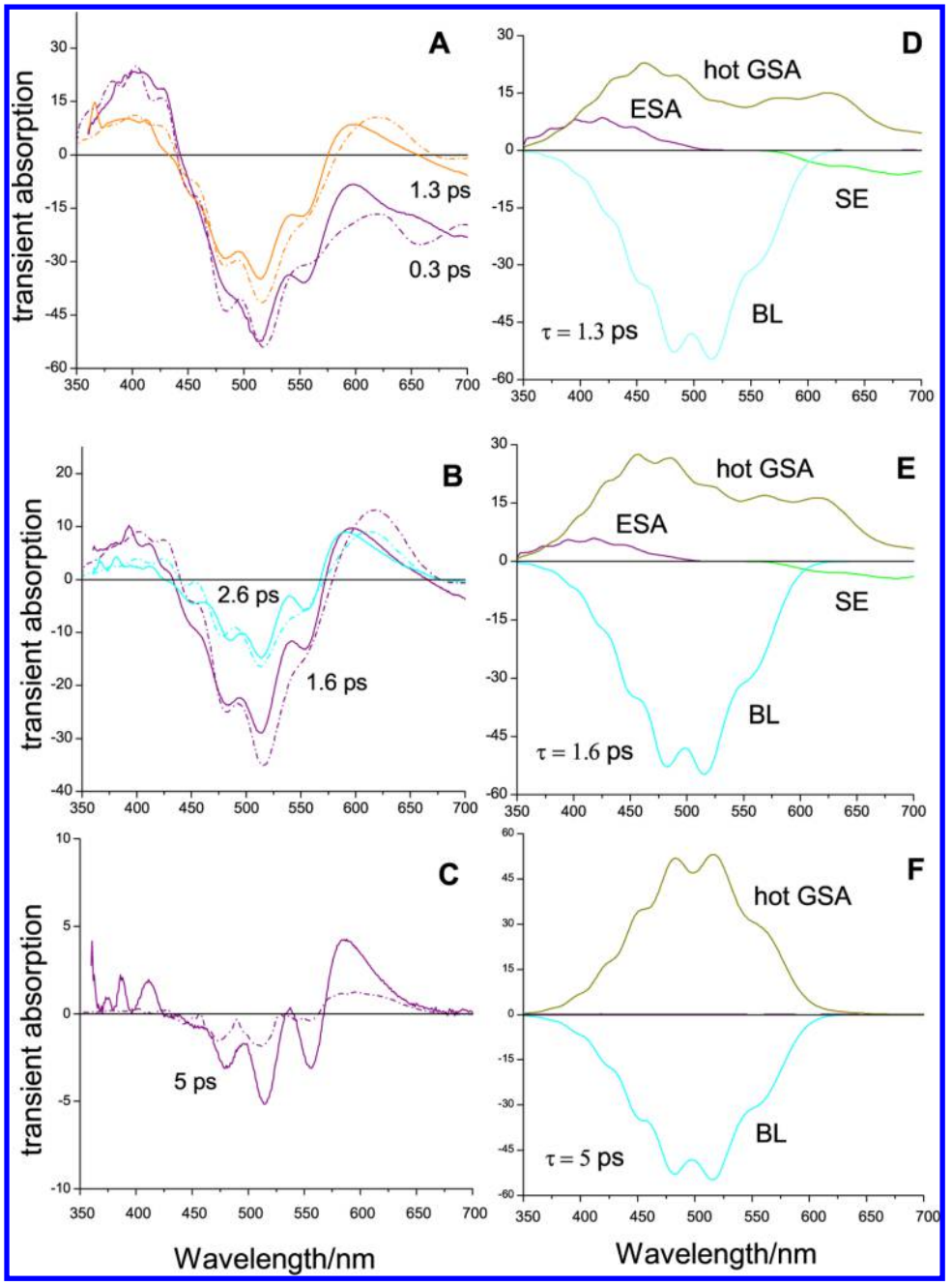

Figure 5. Experimental (solid lines) and simulated (dashed lines) at various time delays after excitation $\Delta A(\lambda)$ (A–C) and their different contributions (D–F). Fitting 2. The parameters are the same as those in Figure 4 except for E_{rmd} = 0.75 eV, x_3 = 0.1, and τ_{vg} = 0.8 ps.

frequency mode. In the framework of this model, the position of this band only could be reproduced if the overall reorganization energy of the low frequency modes for the transitions to the dark state was large. A value of E_{rmd} = 0.75 eV was used in the simulations. The value of ΔG_{ed} = −0.9 eV was chosen to obtain large rate constants for the transitions between the S_1 and the dark states ($e \rightarrow d$) and between the dark and the ground states ($d \rightarrow g$). It appeared that the rate constant of the $e \rightarrow d$ transition has to be considerably smaller than that of the $d \rightarrow g$ transition to ensure that the dark state population remains small at all times. The value of the electronic coupling between the dark and ground states was found to be considerably larger than V_{ed}, namely, V_{dg} = 0.036 eV. Because of the large amount of energy deposited into solvent and intramolecular modes upon both $e \rightarrow d$ and $d \rightarrow g$ transitions, the ground electronic state is repopulated far from equilibrium. Such hot ground-state population appears as a broad positive band in TA spectrum (hot GSA). Although the hot GSA absorption band overlaps with the BL band, its wings appear on both the red and blue sides of the BL band. At long times, e.g., ∼5 ps, the positive TA signal in the blue region of the spectrum is mainly caused by the excitation of high frequency modes, whereas in the red region, the slow structural equilibration of the dyad and the excitation of high frequency modes play a comparable role with the parameters listed in the caption of Figure 6. The simulated hot GSA band becomes considerably narrower if the relaxation time of the high-frequency mode in the S_0 state, τ_v, is reduced (see Figure 4). However, the positive GSA feature on the long-wavelength side of the bleach remains because of the large time constant

DOI: 10.1021/acs.jpca.6b11581
J. Phys. Chem. A 2017, 121, 471–481

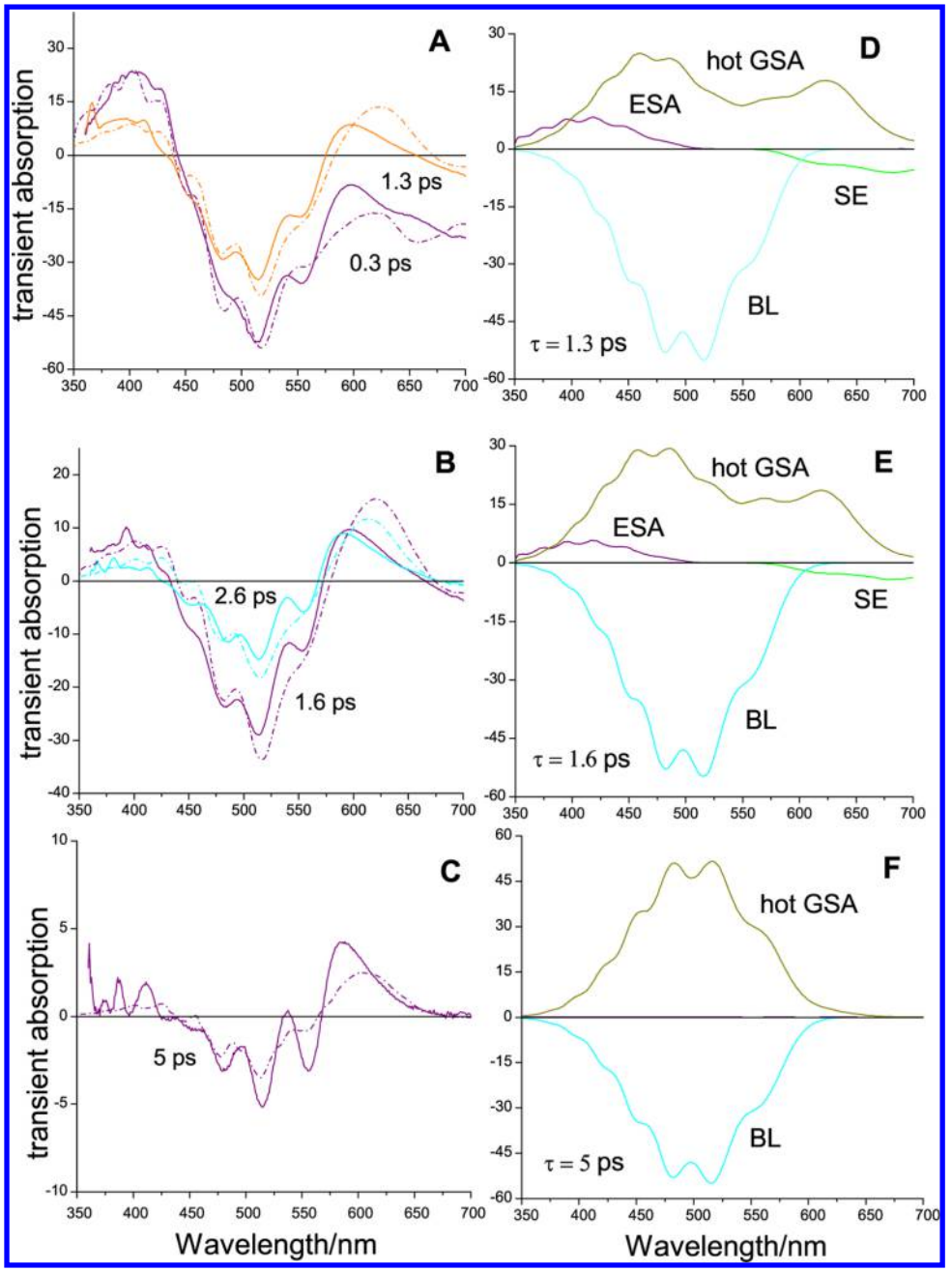

Figure 6. Experimental (solid lines) and simulated (dashed lines) at various time delays after excitation $\Delta A(\lambda)$ (A−C) and their different contributions (D−F). Fitting 3. The parameters are the same as those in Figure 5 except for τ_{vg} = 1.2 ps.

associated with the slowly relaxing mode, τ_3. To understand the origin of the pronounced vibrational structure in the experimental TA spectra at long times (see Figure 4C), the distribution along the reaction coordinate of the molecules having returned to the ground state has to be considered. The $d \rightarrow g$ transition populates the ground state manifold far from the minimum (see Figure 3). The relaxation of this nonequilibrated distribution is not single exponential since it comprises three components with times constant τ_i. The relaxation of the two fast components occurs in parallel with the electronic transitions, whereas the relaxation of the third one is much slower. The population distribution of the molecules just after the electronic transitions is shifted relative to the equilibrium population. Consequently, the hot GSA spectrum including its vibrational structure is red-shifted relative to that of BL. Although this shift is relatively small (see Figure 4F), the overall TA spectrum, being the sum of the hot GSA and BL bands, acquires a pronounced vibrational structure.

The simulated spectra presented in Figures 5 and 6 fit the best at early times when the electronic transitions take place. However, at later times (Figures 5C and 6C) the amplitude of the simulated TA spectrum decays faster than that observed. Since the evolution of the TA spectrum at $t > 2.6$ ps mainly reflects the relaxation of the solvent and high-frequency intramolecular modes, this discrepancy could originate from an incorrect description of vibrational relaxation. The fit can be improved by describing the relaxation of the high-frequency mode with two time constants. The relaxation time depends on the quantum number of the vibrational excited state and is expected to be complex. Unfortunately, experimental informa-

DOI: 10.1021/acs.jpca.6b11581
J. Phys. Chem. A 2017, 121, 471−481

tion on this dependence is absent. The simplest model predicts a $\tau_v^{(n)} = \tau_v^{(1)}/n$ dependence,[65] but better results are obtained with a $\tau_v^{(n)} = \tau_v^{(1)}/n^2$ dependence, as used here in the fitting.

The simulations of the TA spectra were performed assuming the existence of a dark state, which differs from the optically excited state and the ground states by a considerable charge transfer character. Such charge transfer implies a large reorganization energy in polar solvents like ACN. However, the reorganization energy of the solvent for the $e \leftarrow g$ transition is small, and the widths of the stationary and TA bands are predominantly determined by the reorganization of the high frequency mode, E_{rv}. Therefore, the magnitude of E_{rv} can be easily determined from the analysis of the stationary absorption band. With these parameters, both the width and the position of the BL and SE bands can be well reproduced. However, in order to reproduce the observed decay rate of the excited state with such reorganization energies, a free energy gap considerably smaller than ΔG_{eg} has to be assumed. The introduction of the dark state results in 2-fold reduction of the energy gap.

As noted above, the TA spectrum observed in the experiment cannot be reproduced in the framework of a two-level model with the parabolic terms because the fast electronic transitions requires large reorganization energies to be reproduced. As a consequence, the contributions of SE and hot GSA to the simulated TA spectrum exhibit a broad long-wavelength wing extending far beyond 700 nm.[56] At the same time, the two-level model proposed in ref 16 (Figure 7) including a torsional mode

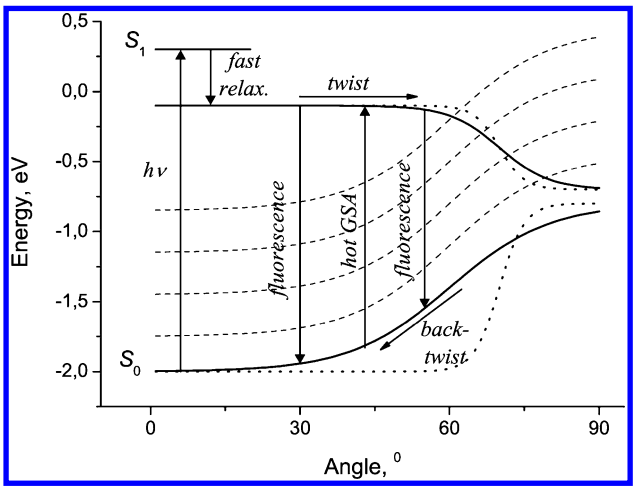

Figure 7. Energy of the S_1 and S_0 states of PP along the reaction coordinate (solid lines, the dashed lines are the excited vibrational sublevels) proposed in ref 16 to account for the excited state dynamics of PP. The curves with dotted lines correspond to the condition required for a short lifetime of the twisted state.

that leads to a strong decrease of the S_1-S_0 energy gap could allow the fast transition to be reproduced. However, such model can face the same problem with the red wing of the spectrum because the twisted molecules have a considerably smaller free energy gap. This problem can be overcome by supposing that either the population of the twisted state is small or this state is dark. This assumption means that the upper and lower free energy curves have to be nearly flat at all twist angles except for a narrow region where the energy changes sharply (dotted lines in Figure 7). Such situation would ensure short lifetime of the twisted state and a TA spectrum localized at very long wavelength, outside the experimental spectral window. Alternatively, the transition dipole moment has to sharply decrease with torsion when the free energy gap starts to decrease. The TA spectra show the important role played by the high-frequency vibrational modes in the electronic transition. As shown by the dashed lines in Figure 7, transitions to vibrational excited state of the electronic ground state can occur at moderate torsion angle.

The good agreement obtained here between the experimental and simulated TA spectra indicates that the difficulties associated with the nonharmonic nature of the free-energy curves along the reaction coordinate can be properly circumvented by using a three-level model, where the additional state is a twisted excited state with considerable different energy and spectroscopic properties from that of the optically excited state.

CONCLUSIONS

A theory of transient absorption spectra of donor−acceptor dyads with ultrafast charge transfer into a dark state has been developed and has been exploited to simulate the spectral dynamics measured with a donor−acceptor biaryl, a pyrylium phenolate, in acetonitrile. The multichannel stochastic model was used to calculate the time-dependent distribution functions. All the most relevant parameters of the model can be determined from the stationary absorption spectrum. The parameters responsible for the excited-state absorption, which only appears at short times, are adjustable. The parameters relevant to the dark state are also adjustable. They control the energy flow from the electronic subsystem to the nuclear degrees of freedom. In order to properly reproduce the fast decay of the optically excited state and the fast ground state recovery, a large reorganization energy of the slow modes is required for the transitions from the excited to the dark state and from the dark to the ground state. This reorganization impacts the spectral dynamics on the red side of the TA spectrum, in particular, the positive signal due to the hot ground state population.

The electronic transitions take place on the subpicosecond time scale, and after approximately 2 ps, the spectral dynamics is only due to the structural relaxation of PP in the ground state. Solvent relaxation is also ultrafast and does not affect the spectral dynamics after 2 ps.

The following conclusions can be drawn from the above results:

1. The simulation of TA spectra provides a possibility to determine the rate constant of photoinduced charge transfer when the contribution of both population changes and relaxation processes to the spectral dynamics are entangled. The excited state lifetime of PP was found to be $\tau = 0.84$ ps, which is close to but differs from that found from the global analysis, $\tau = 0.72$ ps. It should be noted that the excited-state decay is close to exponential so that the lifetime is well-defined.
2. A slowly relaxing mode with a $\tau_3 \approx 5$ ps time constant is needed to reproduce the observed TA spectra. Its relative amplitude is as large $x_3 \approx 0.1-0.3$. This strongly supports the involvement of a torsional mode around the single bond between the donor and acceptor subunits of PP.
3. The transition to the dark state is associated with a large reorganization energy $E_{rm} \approx 1$ eV. This agrees with substantial changes of both the geometry, i.e., torsion,

DOI: 10.1021/acs.jpca.6b11581
J. Phys. Chem. A 2017, 121, 471−481

and the charge-transfer character when going from the optically excited state to the dark state.
4. The relatively large reorganization energy of the high-frequency mode indicates that a considerable amount of the electronic energy is dumped into this mode. The excitation of this mode manifests on the blue side of the bleach band after the decay of the excited-state population.
5. The relaxation time of the high-frequency vibrational mode has a strong influence on the spectral dynamics.

AUTHOR INFORMATION

Corresponding Authors

*E-mail: anatoly.ivanov@volsu.ru.
*E-mail: eric.vauthey@unige.ch.

ORCID

Anatoly I. Ivanov: 0000-0002-4420-5863
Eric Vauthey: 0000-0002-9580-9683

Notes

The authors declare no competing financial interest.

ACKNOWLEDGMENTS

This work was supported by the Russian Science Foundation (Project Nr. 16-13-10122). A.I.I. wishes to thank Swiss National Science Foundation for financial support of his visit to the University of Geneva where an important part of this study was performed (Project Nr. IZK0Z2_166972).

REFERENCES

(1) Blanchard-Desce, M.; Alain, V.; Bedworth, P. V.; Marder, S. R.; Fort, A.; Runser, C.; Barzoukas, M.; Lebus, S.; Wortmann, R. Large Quadratic Hyperpolarizabilities with Donor-Acceptor Polyenes Exhibiting Optimum Bond Length Alternation: Correlation Between Structure and Hyperpolarizability. *Chem. - Eur. J.* **1997**, *3*, 1091−1104.

(2) Boeglin, A.; Barsella, A.; Fort, A.; Mançois, F.; Rodriguez, V.; Diemer, V.; Chaumeil, H.; Defoin, A.; Jacques, P.; Carré, C. Optical Properties and Progressive Sterical Hindering in Pyridinium Phenoxides. *Chem. Phys. Lett.* **2007**, *442*, 298−301.

(3) Kang, H.; Facchetti, A.; Zhu, P.; Jiang, H.; Yang, Y.; Cariati, E.; Righetto, S.; Ugo, R.; Zuccaccia, C.; Macchioni, A.; et al. Exceptional Molecular Hyperpolarizabilities in Twisted π-Electron System Chromophores. *Angew. Chem., Int. Ed.* **2005**, *44*, 7922−7925.

(4) Isborn, C. M.; Davidson, E. R.; Robinson, B. H. Ab Initio Diradical/Zwitterionic Polarizabilities and Hyperpolarizabilities in Twisted Double Bonds. *J. Phys. Chem. A* **2006**, *110*, 7189−7196.

(5) Kang, H.; Facchetti, A.; Jiang, H.; Cariati, E.; Righetto, S.; Ugo, R.; Zuccaccia, C.; Macchioni, A.; Stern, C. L.; Liu, Z.; et al. Ultralarge Hyperpolarizability Twisted π-Electron System Electro-Optic Chromophores: Synthesis, Solid-State and Solution-Phase Structural Characteristics, Electronic Structures, Linear and Nonlinear Optical Properties, and Computational Studies. *J. Am. Chem. Soc.* **2007**, *129*, 3267−3286.

(6) Liu, L.; Xue, Y.; Wang, X.; Chu, X.; Yang, M. Theoretical Study of Static (Hyper)polarizabilities of Twisted Intramolecular Charge Transfer Chromophores. *Int. J. Quantum Chem.* **2012**, *112*, 1086−1096.

(7) Barbara, P. F.; Walker, G. C.; Smith, T. P. Vibrational Modes and the Dynamic Solvent Effect in Electron and Proton Transfer. *Science* **1992**, *256*, 975−981.

(8) Johnson, A. E.; Levinger, N. E.; Jarzeba, W.; Schlief, R. E.; Kliner, D. A. V.; Barbara, P. F. Experimental and Theoretical Study of Inhomogeneous Electron Transfer in Betaine: Comparison of Measured and Predicted Spectral Dynamics. *Chem. Phys.* **1993**, *256*, 555−574.

(9) Reid, P. J.; Barbara, P. F. Dynamic Solvent Effect on Betaine-30 Electron Transfer Kinetics in Alcohols. *J. Phys. Chem.* **1995**, *99*, 3554−3565.

(10) Lobaugh, J.; Rossky, P. J. Computer Simulation of the Excited State Dynamics of Betaine-30 in Acetonitrile. *J. Phys. Chem. A* **1999**, *103*, 9432−9447.

(11) Kovalenko, S. A.; Eilers-König, N.; Senyushkina, T.; Ernsting, N. P. Charge Transfer and Solvation of Betaine-30 in Polar Solvents: A Femtosecond Broadband Transient Absorption Study. *J. Phys. Chem. A* **2001**, *105*, 4834−4843.

(12) Ishida, T.; Rossky, P. J. Consequences of Strong Coupling between Solvation and Electronic Structure in the Excited State of a Betaine Dye. *J. Phys. Chem. B* **2008**, *112*, 11353−11360.

(13) Kharlanov, V.; Rettig, W. Experimental and Theoretical Study of Excited-State Structure and Relaxation Processes of Betaine-30 and of Pyridinium Model Compounds. *J. Phys. Chem. A* **2009**, *113*, 10693−10703.

(14) Duvanel, G.; Grilj, J.; Chaumeil, H.; Jacques, P.; Vauthey, E. Ultrafast Excited-State Dynamics of a Series of Zwitterionic Pyridinium Phenoxides with Increasing Sterical Hindering. *Photochem. Photobiol. Sci.* **2010**, *9*, 908−915.

(15) Malval, J.-P.; Chaumeil, H.; Rettig, W.; Kharlanov, V.; Diemer, V.; Ay, E.; Morlet-Savary, F.; Poizat, O. Excited-State Dynamics of Phenol-Pyridinium Biaryl. *Phys. Chem. Chem. Phys.* **2012**, *14*, 562−574.

(16) Letrun, R.; Koch, M.; Dekhtyar, M. L.; Kurdyukov, V. V.; Tolmachev, A. I.; Rettig, W.; Vauthey, E. Ultrafast Excited-State Dynamics of Donor-Acceptor Biaryls: Comparison between Pyridinium and Pyrylium Phenolates. *J. Phys. Chem. A* **2013**, *117*, 13112−13126.

(17) Van Stokkum, I. H. M.; Larsen, D. S.; van Grondelle, R. Global and Target Analysis of Time-Resolved Spectra. *Biochim. Biophys. Acta, Bioenerg.* **2004**, *1657*, 82−104.

(18) Mukamel, S. *Nonlinear Optical Spectroscopy*; Oxford University Press: New York, 1995; p 544.

(19) Domcke, W.; Stock, G. Theory of Ultrafast Nonadiabatic Excited State Processes and Their Spectroscopic Detection in Real Time. *Adv. Chem. Phys.* **1997**, *100*, 1−168.

(20) Koch, C. P.; Klüner, T.; Kosloff, R. A Complete Quantum Description of an Ultrafast Pump-Probe Charge Transfer Event in Condensed Phase. *J. Chem. Phys.* **2002**, *116*, 7983−7996.

(21) Joo, T.; Jia, Y.; Yu, J.-Y.; Lang, M. J.; Fleming, G. R. Third-Order Nonlinear Time Domain Probes of Solvation Dynamics. *J. Chem. Phys.* **1996**, *104*, 6087−6108.

(22) Egorova, D.; Gelin, M. F.; Domcke, W. Time- and Frequency-Resolved Fluorescence Spectra of Nonadiabatic Dissipative Systems: What Photons Can Tell Us. *J. Chem. Phys.* **2005**, *122*, 134504.

(23) Rosspeintner, A.; Lang, B.; Vauthey, E. Ultrafast Photochemistry in Liquids. *Annu. Rev. Phys. Chem.* **2013**, *64*, 247−271.

(24) Kuznetsov, A. M. *Charge Transfer in Physics, Chemistry and Biology*; Gordon & Breach: Amsterdam, 1995; p 622.

(25) Jortner, J., Bixon, M., Eds. *Electron Transfer: From Isolated Molecules to Biomolecules*; Wiley, 2007.

(26) Barzykin, A. V.; Frantsuzov, P. A.; Seki, K.; Tachiya, M. Solvent Effects in Nonadiabatic Electron-Transfer Reactions: Theoretical Aspects. *Adv. Chem. Phys.* **2002**, *123*, 511−616.

(27) Ivanov, A. I.; Mikhailova, V. A. Kinetics of Fast Photochemical Charge Separation and Charge Recombination Reactions. *Russ. Chem. Rev.* **2010**, *79*, 1047−1070.

(28) Tully, J. C. Molecular Dynamics with Electronic Transitions. *J. Chem. Phys.* **1990**, *93*, 1061−1071.

(29) Li, Z.; Fang, J. Y.; Martens, C. C. Simulation of Ultrafast Dynamics and Pump-Probe Spectroscopy Using Classical Trajectories. *J. Chem. Phys.* **1996**, *104*, 6919−6929.

(30) Yang, D.-Y.; Sheu, S.-Y. Pump-Probe Spectroscopy of Photoinduced Charge Transfer Reactions in Solution. *J. Chem. Phys.* **1997**, *106*, 9427−9438.

(31) Hartmann, M.; Pittner, J.; Bonačić-Koutecký, V.; Heidenreich, A.; Jortner, J. Ultrafast Dynamics of Small Clusters on the Time Scale of Nuclear Motion. *J. Phys. Chem. A* **1998**, *102*, 4069−4074.

DOI: 10.1021/acs.jpca.6b11581
J. Phys. Chem. A 2017, 121, 471−481

(32) Hartmann, M.; Pittner, J.; Bonačić-Koutecký, V. Ab Initio Adiabatic Dynamics Involving Excited States Combined with Wigner Distribution Approach to Ultrafast Spectroscopy Illustrated on Alkali Halide Clusters. *J. Chem. Phys.* **2001**, *114*, 2106−2122.
(33) Hartmann, M.; J, P.; Bonačić-Koutecký, V. Ab Initio Nonadiabatic Dynamics Involving Conical Intersection Combined with Wigner Distribution Approach to Ultrafast Spectroscopy Illustrated on Na_3F_2 Cluster. *J. Chem. Phys.* **2001**, *114*, 2123−2136.
(34) Bonačić-Koutecký, V.; Mitrić, R. Theoretical Exploration of Ultrafast Dynamics in Atomic Clusters: Analysis and Control. *Chem. Rev.* **2005**, *105*, 11−66.
(35) Lindinger, A.; Bonačić-Koutecký, V.; Mitric, R.; Tannor, D.; Koch, C. P.; Engel, V.; Bernhardt, T. M.; Jortner, J.; Mirabal, A.; Woste, L. Analysis and Control of Small Isolated Molecular Systems. *Springer Series in Chemical Physics* **2007**, *87*, 25−152.
(36) Barbatti, M.; Granucci, G.; Persico, M.; Ruckenbauer, M.; Vazdar, M.; Eckert-Maksi, M.; Lischka, H. The On-the-Fly Surface-Hopping Program System Newton-X: Application to Ab Initio Simulation of the Nonadiabatic Photodynamics of Benchmark Systems. *J. Photochem. Photobiol., A* **2007**, *190*, 228−240.
(37) Egorova, D.; Gelin, M. F.; Thoss, M.; Wang, H.; Domcke, W. Effects of Intense Femtosecond Pumping on Ultrafast Electronic-Vibrational Dynamics in Molecular Systems with Relaxation. *J. Chem. Phys.* **2008**, *129*, 214303.
(38) De Giovannini, U.; Brunetto, G.; Castro, A.; Walkenhorst, J.; Rubio, A. Simulating Pump−Probe Photoelectron and Absorption Spectroscopy on the Attosecond Timescale with Time-Dependent Density Functional Theory. *ChemPhysChem* **2016**, *14*, 1363−1376.
(39) Fischer, S. A.; Cramer, C.; Govind, N. Excited State Absorption from Real-Time Time-Dependent Density Functional Theory. *J. Chem. Theory Comput.* **2015**, *11*, 4294−4303.
(40) Nguyen, T. S.; Koh, J. H.; Lefelhocz, S.; Parkhill, J. Black-Box, Real-Time Simulations of Transient Absorption Spectroscopy. *J. Phys. Chem. Lett.* **2016**, *7*, 1590−1595.
(41) Bagchi, B.; Gayathri, N. Interplay Between Ultrafast Polar Solvation and Vibrational Dynamics in Electron Transfer Reactions: Role of High-Frequency Vibrational Modes. *Adv. Chem. Phys.* **1999**, *107*, 1−80.
(42) Feskov, S. V.; Ionkin, V. N.; Ivanov, A. I. Effect of High-Frequency Modes and Hot Transitions on Free Energy Gap Dependence of Charge Recombination. *J. Phys. Chem. A* **2006**, *110*, 11919−11925.
(43) Feskov, S. V.; Ionkin, V. N.; Ivanov, A. I.; Hagemann, H.; Vauthey, E. Solvent and Spectral Effects in the Ultrafast Charge Recombination Dynamics of Excited Donor-Acceptor Complexes. *J. Phys. Chem. A* **2008**, *112*, 594−601.
(44) Nazarov, A. E.; Fedunov, R. G.; Ivanov, A. I. Principals of Simulation of Ultrafast Charge Transfer in Solution within the Multichannel Stochastic Point-Transition Model. *Comput. Phys. Commun.* **2017**, *210*, 172−180.
(45) Feskov, S. V.; Mikhailova, V. A.; Ivanov, A. I. Non-equilibrium effects in ultrafast photoinduced charge transfer kinetics. *J. Photochem. Photobiol., C* **2016**, *29*, 48−72.
(46) Yudanov, V. V.; Mikhailova, V. A.; Ivanov, A. I. Nonequilibrium Phenomena in Charge Recombination of Excited Donor-Acceptor Complexes and Free Energy Gap Law. *J. Phys. Chem. A* **2010**, *114*, 12998−13004.
(47) Yudanov, V. V.; Mikhailova, V. A.; Ivanov, A. I. Reorganization of Intramolecular High Frequency Vibrational Modes and Dynamic Solvent Effect in Electron Transfer Reactions. *J. Phys. Chem. A* **2012**, *116*, 4010−4019.
(48) Mikhailova, T. V.; Mikhailova, V. A.; Ivanov, A. I. Dynamic Solvent Effect on Ultrafast Charge Recombination Kinetics in Excited Donor-Acceptor Complexes. *J. Phys. Chem. B* **2016**, *120*, 11987−11995.
(49) Marcus, R. A. On the Theory of Oxidation-Reduction Reactions Involving Electron Transfer. *J. Chem. Phys.* **1956**, *24*, 966−978.
(50) Schenck, C. C.; Parson, W. W.; Holten, D.; Windsor, M. W.; A, S. Temperature Dependence of Electron Transfer between Bacteriopheophytin and Ubiquinone in Protonated and Deuterated Reaction Centers of Rhodopseudomonas Sphaeroides. *Biophys. J.* **1981**, *36*, 479−489.
(51) Gunner, M. R.; Robertson, D. E.; Dutton, P. L. Kinetic Studies on the Reaction Center Protein from Rhodopseudomonas Sphaeroides: the Temperature and Free Energy Dependence of Electron Transfer between Various Quinones in the QA Site and the Oxidized Bacteriochlorophyll Dimer. *J. Phys. Chem.* **1986**, *90*, 3783−3795.
(52) Schmid, R.; Labahn, A. Temperature and Free Energy on the Direct Charge Recombination Rate from the Secondary Quinone in Bacterial Reaction Centers from Rhodobacter Sphaeroides. *J. Phys. Chem. B* **2000**, *104*, 2928−2936.
(53) Kang, Y. K.; Duncan, T. V.; Therien, M. J. Temperature-Dependent Mechanistic Transition for Photoinduced Electron Transfer Modulated by Excited-State Vibrational Relaxation Dynamics. *J. Phys. Chem. B* **2007**, *111*, 6829−6838.
(54) Wang, H.; Lin, S.; Katilius, E.; Laser, C.; Allen, J. P.; Williams, J. C.; Woodbury, N. W. Unusual Temperature Dependence of Photosynthetic Electron Transfer due to Protein Dynamics. *J. Phys. Chem. B* **2009**, *113*, 818−824.
(55) Rogozina, M. V.; Ionkin, V. N.; Ivanov, A. I. Dynamics of Charge Separation from Second Excited State and Following Charge Recombination in Zinc-Porphyrin-Acceptor Dyads. *J. Phys. Chem. A* **2013**, *117*, 4564−4573.
(56) Fedunov, R. G.; Plotnikova, A. V.; Ionkin, V. N.; Ivanov, A. I. Dynamics of Ground State Absorption Spectra in Donor-Acceptor Pairs with Ultrafast Charge Recombination. *J. Phys. Chem. A* **2015**, *119*, 1964−1972.
(57) Rosenthal, S. J.; Xie, X.; Du, M.; Fleming, G. Femtosecond Solvation Dynamics in Acetonitrile: Observation of the Inertial Contribution to the Solvent Response. *J. Chem. Phys.* **1991**, *95*, 4715−4718.
(58) Maroncelli, M.; Kumar, V. P.; Papazyan, A. A Simple Interpretation of Polar Solvation Dynamics. *J. Phys. Chem.* **1993**, *97*, 13−17.
(59) Jimenez, R.; Fleming, G. R.; Kumar, P. V.; Maroncelli, M. Femtosecond Solvation Dynamics of Water. *Nature* **1994**, *369*, 471−473.
(60) Zusman, L. D. Outer-Sphere Electron Transfer in Polar Solvents. *Chem. Phys.* **1980**, *49*, 295−304.
(61) Fedunov, R. G.; Feskov, S. V.; Ivanov, A. I.; Nicolet, O.; Pagès, S.; Vauthey, E. Effect of the Excitation Pulse Carrier Frequency on the Ultrafast Charge Recombination Dynamics of Donor-Acceptor Complexes: Stochastic Simulations and Experiments. *J. Chem. Phys.* **2004**, *121*, 3643−3656.
(62) Gladkikh, V.; Burshtein, A. I.; Feskov, S. V.; Ivanov, A. I.; Vauthey, E. Hot Recombination of Photogenerated Ion Pairs. *J. Chem. Phys.* **2005**, *123*, 244510.
(63) Horng, M. L.; Gardecki, J. A.; Papazyan, A.; Maroncelli, M. Subpicosecond Measurements of Polar Solvation Dynamics: Coumarin 153 Revisited. *J. Phys. Chem.* **1995**, *99*, 17311−17337.
(64) Kharlanov, V.; Rettig, W. Experimental and Theoretical Study of Excited-State Structure and Relaxation Processes of Betaine-30 and of Pyridinium Model Compounds. *J. Phys. Chem. A* **2009**, *113*, 10693−10703.
(65) Ivanov, A.; Ionkin, V.; Feskov, S. Acceleration of the Recombination of Photoexcited Donor-Acceptor Complexes with a High-Frequency Vibrational Mode. *Russ. J. Phys. Chem. A* **2008**, *82*, 303−309.

DOI: 10.1021/acs.jpca.6b11581
J. Phys. Chem. A 2017, 121, 471−481